IEEE Access
Multidisciplinary | Rapid Review | Open Access Journal

Received November 22, 2017, accepted December 14, 2017, date of publication December 19, 2017, date of current version February 14, 2018.

Digital Object Identifier 10.1109/ACCESS.2017.2785322

Prediction of Lung Motion From Four-Dimensional Computer Tomography (4DCT) Images Using Bayesian Registration and Trajectory Modelling

MIN LI[1], ZHIKANG XIANG[1], ZHICHAO LIAN[1], LIANG XIAO[1], (Member, IEEE), JUN ZHANG[2], AND ZHIHUI WEI[1]

[1]School of Computer Science and Engineering, Nanjing University of Science and Technology, Nanjing 210094, China
[2]School of Science, Nanjing University of Science and Technology, Nanjing 210094, China

Corresponding author: Min Li (limin_022@163.com)

This work was supported in part by the National Natural Science Foundation of China under Grant 61501241 and Grant 61671243, in part by the Natural Science Foundation of Jiangsu Province under Grant BK20 150792, and in part by the China Postdoctoral Science Foundation under Grant 2015 M570450.

ABSTRACT Respiratory motion causes difficulty in locating tumours in the thorax and upper abdomen for image-guided radiotherapy. Precisely predicting the respiratory-induced organ motion is still a challenging problem at present. In this paper, to predict the motion of lungs in a respiratory cycle, we propose a novel method comprising Bayesian registration and trajectory modelling based on cine four-dimensional computer tomography (4DCT) images. Specifically, we take the CT image captured at the end-inhale phase as the source image and those captured at other phases as the moving images. We then align the source image to each moving-phase image to generate the displacement fields using the Bayesian registration method. The lung-motion trajectory is then modelled based on a continuous time-related displacement field by linking the displacement fields at discrete phases. The results indicate that any point in the lungs at any given time is accurately predicted using the proposed method, which provides an alternative method of estimating the lung and tumour motions for radiation therapy.

INDEX TERMS Bayesian method, computer tomography, image registration, lung motion.

I. INTRODUCTION

Respiratory motion induces uncertainties in the shape, volume, and location of a tumour, making it difficult to conduct image-guided radiotherapy of tumours in the thorax and upper abdomen regions [1], [2]. Actually, all organs in the thorax and abdomen suffer from such uncertainties due to respiratory motion, among which the lung is most affected. Hence, respiratory motion management is of great significance in lung cancer radiotherapy.

Some techniques have been used for motion management, such as breath-hold methods, abdominal compression, respiratory tracking and respiratory gating [3]. However, breath-hold techniques and abdominal compression may not be suitable for patients with poor respiratory function. Respiratory tracking and gating relies on the interpretation of either internal or external surrogates. Radio-opaque fiducials are often used as internal surrogates but prone to pitfalls such as the risk of pneumothorax and marker migration [3]. Although some signals have been used as external surrogates to estimate the motion of the lungs, these signals are often obtained using devices such as spirometers, abdominal pressure belts, and external markers, which are limited in reflecting the complexity of the lung motion. Four-dimensional computed tomography (4DCT) comprises a sequence of 3D images captured at different periods in a breathing cycle, making it possible to visualise the motion of a tumour. This method has been widely used to aid radiation treatment planning [4] and have potential improving the therapeutic window with motion management [5].

One of the easier methods involves determining the deformation of the lung by tracking the region of interest (ROI) across the 4DCT images, which requires establishing a

correspondence between the different respiratory states of the lungs. Considering the objective of image registration is to obtain a transformation by aligning the features of one image with the correspondences of another image, registration algorithms can be used to detect and quantify the deformation in the lungs from the serial images.

Existing registration methods can be categorised into rigid registration and non-rigid registration approaches [6]. Compared to the rigid registration wherein only translation and rotational motions are applied for transformations, the non-rigid registration is more suitable for representing the complicated deformation and distortion of the anatomy. Various non-rigid registration algorithms have been developed for medical images and can be divided into feature-based algorithms [7]–[10], intensity-based approaches [11]–[13], and physical models [14]–[17].

The feature-based methods are widely used in the medical field. For instance, Xiong *et al.* [18] detected junction structures as landmarks in the lungs and modelled the lung motion based on their trajectories using a B-spline method. However, extracting the landmarks is time consuming and prone to bias. In the intensity-based methods, the intensity information is directly used without extracting the features for image registration. In many of the intensity-based algorithms such as the optical-flow method [19] and the sum of squared difference method [20], the intensity of an image is assumed to be conserved, which is not true in reality because the respiratory motion causes variation in the intensity of the images of the lungs. The physical models describe the lung motion as a physical process. One of the widely used physical models is the biomechanical model [15], [21]. The lungs are simply modelled to be uniform in the reported biomechanical approaches because of the lack of material properties, which is not true in reality and limits the applications.

To address the aforementioned limitations, we propose a generative-respiratory model to predict the lung motion in this study, which contrary to previous approaches is based on patient-specific 4DCT images. The proposed method comprises two stages: Bayesian registration and trajectory modelling. The correspondence between the different respiratory states of the lungs at different time is determined using Bayesian registration so that the spatiotemporal motion can be constructed via trajectory modelling.

The main contributions of this study are in (1) having developed an algorithm based on Bayesian registration and trajectory modelling, which not only can have a comparable registration performance to the state-of-the-art deformable registration methods but also can predict the lung positions at any given time in a respiratory cycle, and (2) having demonstrated that the proposed method has the potential to be used for radiation therapy through estimating lung and tumour motions.

II. PROPOSED METHODOLOGY

In this study, we propose a method of estimating the motion of the patient-specific lung from serial 4DCT data using the Bayesian non-rigid registration and trajectory modelling. The Bayesian registration is employed to align the sequential 4DCT phase images of the lungs, given in section *A*, which produces a dense deformation field with displacement information at every phase. Using these deformation fields, we designed a trajectory function to simulate the motion of the lungs during respiration, given in section *B*. The implementation of the proposed algorithm is introduced in section *C*.

A. BAYESIAN REGISTRATION

We make the following assumptions to align the moving images with a source image. Assuming that x is a point in the source image and y is the corresponding point in the moving image, the displacement vector u_x between them satisfies the equation $y = x + u_x$. Thus, we describe the image registration as a problem of searching for an underlying displacement field such that the ROI in the source image is aligned optimally with the correspondence of the moving image.

The optimal displacements can be obtained by minimising a cost function E comprising an image similarity term E_s and a regularisation term E_r where $E = E_s + E_r$. This framework is independent of the specific forms of the similarity term, regularisation term, or transformation model.

Assuming S and M as the source and moving images, respectively, the relationship between the moving and source images can be modelled as follows.

$$M = S \circ U + \eta \tag{1}$$

where U is the displacement field, and η is the noise.

In a Bayesian framework for registration [22], the displacement field U can be evaluated by maximising their posterior probability as follows.

$$\begin{aligned} P(U|M,S) &= \frac{P(M|U,S)\,P(U)}{P(M)} \\ &\propto P(M|U,S)\,P(U) \end{aligned} \tag{2}$$

where $P(M|U,S)$ is the data likelihood representing the probability of observing the moving image with the deformation U under the noise model in Eq. (1). $P(U)$ means the prior that contributes additional information to regularise the ill-posed maximum likelihood problem. The best estimate U satisfies the maximum posterior criterion, which can be used to minimise the cost function as follows.

$$\begin{aligned} E(U) &= \text{-log}\{P(U|M,S)\} \\ &\propto -\log P(M|U,S)P(U) \\ &= -\{\log P(M|U,S) + \log P(U)\} \end{aligned} \tag{3}$$

Here, the cost function E comprises an image-dissimilarity term $E_s = -\log P(M|U,S)$ and a regularisation term $E_r = -\log P(U)$.

We assume that the noise is modelled using a Gaussian distribution $N(\mu, \delta^2)$ for each local region Ω_ℓ in image. Moreover, the voxels are independent and identically distributed

(i.i.d.) which allows breaking down the global data likelihood into a product of point-wise conditional probabilities as follows.

$$P(M|U,S) = \prod_{\ell}\prod_{x\in\Omega_\ell} P(M(x+u_x)|u,S(x)) = \prod_{\ell}\prod_{x\in\Omega_\ell} \frac{1}{\sqrt{2\pi\delta^2}} e^{(-\frac{(M(x+u_x)-S(x)-\mu)^2}{2\delta})} \quad (4)$$

Therefore,

$$E_s = -\log(\prod_{\ell}\prod_{x\in\Omega_\ell} \frac{1}{\sqrt{2\pi\delta^2}} e^{(-\frac{(M(x+u_x)-S(x)-\mu)^2}{2\delta})}) \propto \sum_{\ell}\sum_{x\in\Omega_\ell} (M(x+u_x)-S(x)-\mu)^2 \quad (5)$$

where μ is the mean change in the grey value of pixels in the local region Ω_ℓ, which is computed based on the sum of squared difference between the local regions as $\mu = 1/N_{\Omega_\ell} \sum_{x\in\Omega_\ell} (M(x+u_x)-S(x))$. N_{Ω_ℓ} is the number of voxels in the region Ω_ℓ.

Given that X voxels exist in the source image, we assume that the displacement field U can be considered random variables and approximately represented using a transformation function.

$$U = AX + B + \varepsilon \quad (6)$$

where A and B are the transformation matrices with parameters $a_j\,(j=1,2,3...9)$ and $b_i\,(i=1,2,3)$ defined as $A = \begin{bmatrix} a_1\text{-}1 & a_2 & a_3 \\ a_4 & a_5-1 & a_6 \\ a_7 & a_8 & a_9-1 \end{bmatrix}$, *and* $B = \begin{bmatrix} b_1 \\ b_2 \\ b_3 \end{bmatrix}$, respectively. ε is called the transformation error, which is modelled using a standard Gaussian distribution. Therefore, we can obtain the regularisation term as follows.

$$E_r = -\log P(U) \propto \sum_{x\in\ell} (u_x - Ax - B)^2 \quad (7)$$

So far, we established the cost function E comprising the data similarity and displacement regularisation terms by minimising $E_s + E_r$, which is defined simply using the unknown displacement vectors and transformation parameters.

B. TRAJECTORY MODELLING

We model the lung motion based on the time-continuous displacement field using a cubic polynomial function such that the image voxel position can be located in 3D space at any given time in a respiratory cycle. The time-continuous displacement function is defined as follows.

$$\begin{bmatrix} u_1(t) \\ u_2(t) \\ u_3(t) \end{bmatrix} = \begin{bmatrix} q_1 & q_2 & q_3 & q_4 \\ q_5 & q_6 & q_7 & q_8 \\ q_9 & q_{10} & q_{11} & q_{12} \end{bmatrix} \begin{bmatrix} t^3 & t^2 & t & 1 \end{bmatrix}^{\mathrm{T}} \quad (8)$$

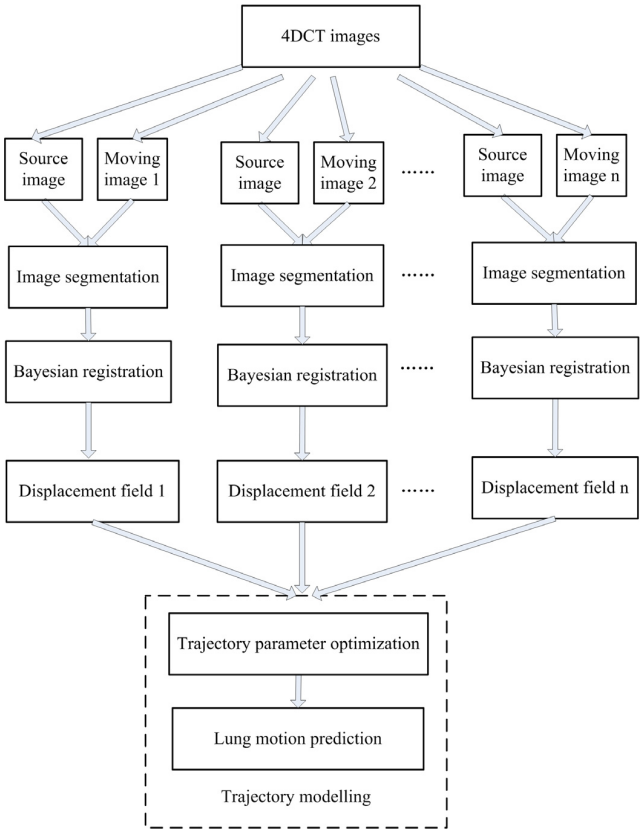

FIGURE 1. Framework of the proposed method.

where $q_j\,(j=1,2,3...12)$ are the trajectory-fitting parameters. $u_i\,(t)\,(i=1,2,3)$ are the displacement components at time t in the x, y, and z directions, respectively.

C. ALGORITHM IMPLEMENTATION

In this study, we reconstruct the continuous displacement field to model the motion of the lungs during a respiratory cycle using 4DCT images. Figure 1 shows the framework of the proposed method that is implemented and described as follows.

1) *Image pre-processing*. Given 4DCT images, we consider the CT image from a particular phase as the source image and each image from other phases as the moving image. We then extract lung regions from CT images using the method introduced in [23].
2) *Bayesian registration*. Align the source image to each moving image for establishment of the corresponding displacement fields between the different phases using Bayesian registration. Specifically, to obtain the optimal displacement field, we divide the Bayesian registration process into two stages based on minimising the data similarity term and the displacement regularisation term. In the first stage, we consider the similarity term in Eq.(5) as the registration metric and employ the neighbourhood of a voxel to form its local region. We then use a block-matching approach to determine

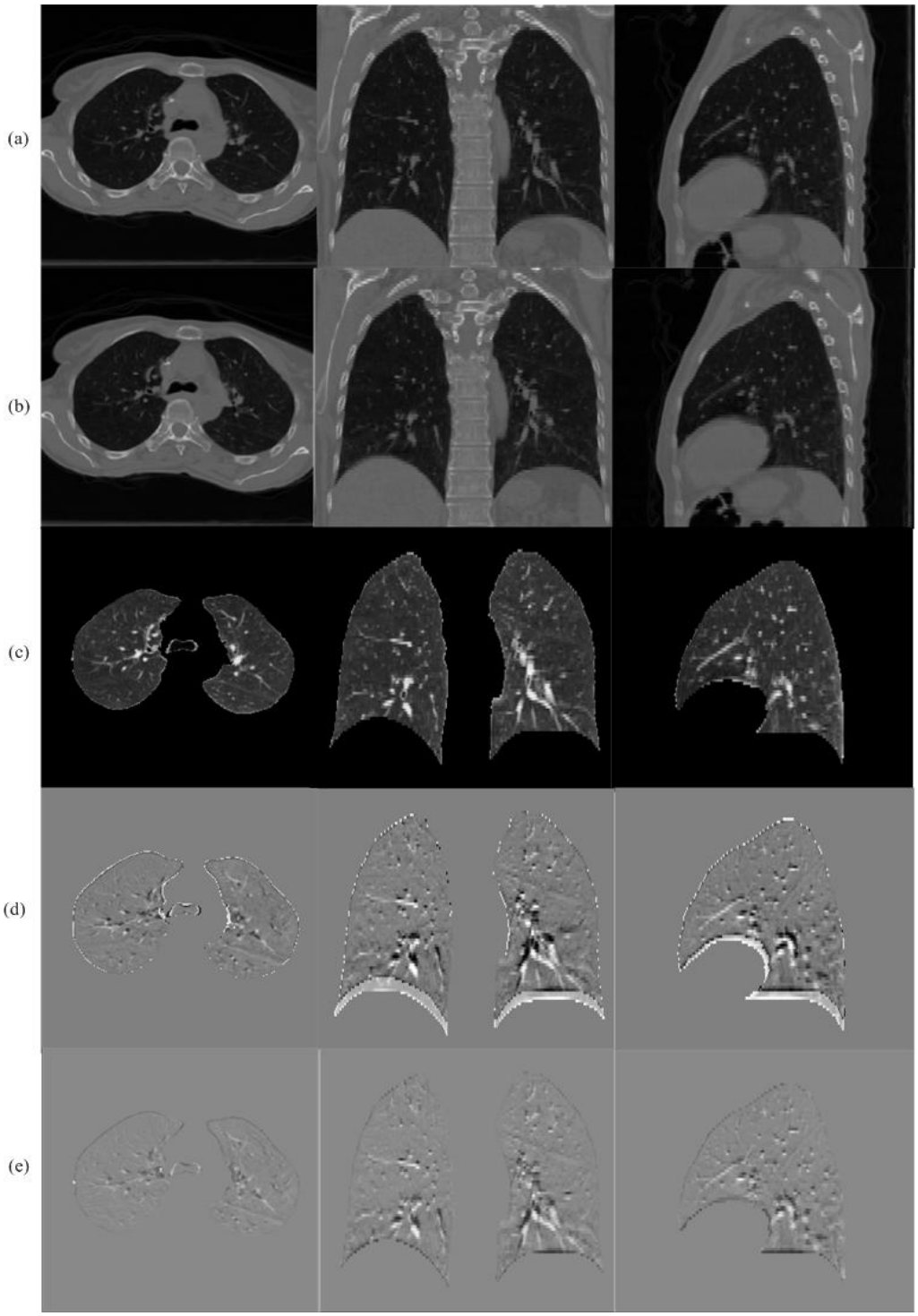

FIGURE 2. Prediction results of lung motion from representative CT images presented in axial, coronal, and sagittal views, respectively: (a) source images, (b) moving images, (c) prediction results, (d) subtraction images showing the difference between lungs in (a) and (b) with no prediction, and (e) subtraction images showing the difference between the lungs in (a) and (b) after prediction using the proposed method.

the displacement vector for each voxel by minimising the registration metric. In the second stage, the optimal transformation parameters a_j $(j = 1, 2, 3...9)$ and b_i $(i = 1, 2, 3)$ in Eq (7) can be calculated using a simple process based on the least median of the square filter [24]. Firstly, all the points in the source image and their corresponding displacement vectors obtained from the first stage are used to initialise m (m =9+3)

parameters and the displacement residual is obtained for each point. Secondly, the parameters a_j and b_i are updated using m + 1 points with the m + 1smallest residuals until all the points are included. Finally, only displacement vectors leading to the lowest median of the residuals are maintained and used to compute the optimal parameters such that the entire smooth displacement field is obtained by interpolation.

3) *Trajectory modelling*. Estimate the parameters given in Eq.(8) using the least-squared method with displacement fields obtained from the Bayesian registration. Accordingly, the respiratory motion of the lungs is modelled based on the continuous displacement field, allowing for the prediction of any point in the lungs at any given time in a respiratory cycle.

III. RESULTS

In this study, the 4DCT images were obtained using a cine 4DCT imaging model, which was provided by the Deformable Image Registration Laboratory of the University of Texas MD Anderson Cancer Center. The acquired images have been retrospectively phase sorted into 10 bins, each of which are equally spaced in time over the breathing cycle. The 10 bins ranged from T00 to T90 with an equal interval, among which T00 and T50 correspond to the end inhale and end exhale phases, respectively. We randomly selected the 4DCT images of six patients to conduct the experiment. Table 1 lists the data characteristics.

We consider the CT image captured at the end-inhale phase as the source image and each image captured at other phases as the moving images for image registration. We then model the motion of the lungs using the proposed method. Fig. 2 shows the predicted results of the lung motion with the help of the representative CT images presented in axial, coronal, and sagittal views, respectively. To illustrate the difference between the ROIs, the subtracted images with and without prediction are given for comparison, as shown in Fig. 2. The subtracted images show a clear decrease in the overall error in the lung boundary using the proposed method compared to the no-prediction case, indicating that the proposed method is effective in prediction of lung motion.

To validate the accuracy of the proposed method, we measure the error in evaluating the deformation of the lungs using landmarks, which have been determined by medical experts. Table 2 presents the details of the landmarks used in experiment. Figure 3 illustrates error vectors of landmarks between T00 and T50 for case 2 prior to registration, and after registration using the Bayesian registration and the proposed trajectory model. The error vectors are obviously seen before registration and substantially decreased after registration using either the Bayesian registration or the proposed trajectory model.

For each patient, we measure the mean prediction error and standard deviation (SD) along the anterior–posterior (AP), left–right (LR), and superior–inferior (SI) directions, respectively, and compare them with those obtained using the linear-trajectory prediction model [25] and the cosine-trajectory model [26]. Results are shown in Table 3. The overall mean errors ±SD for the linear trajectory model, the cosine trajectory model and the proposed method are 3.70 ± 5.26 mm, 1.25 ± 0.81 mm and 1.09 ± 0.68 mm, respectively. Moreover, along each of the AP, LR, and SI directions, the proposed method yields a lower mean error than the linear and cosine models, which shows that the proposed method is more accurate in predicting the motion of lungs.

To evaluate the accuracy of the proposed method in lung motion estimation, we further compare our result with that of four state-of-the-art non-rigid registration methods, including the Demons based method [27], the anatomically constrained deformation algorithm (ANACONDA) based method [28] and the biomechanical model [29], as well as the symmetric registration approach [30]. Table 4 shows the mean error and SD over 300 landmarks for each patient by using different methods. The mean errors ±SD of registration are

TABLE 1. Characteristics of the 4DCT data used in experiment.

C	RP (s)	TV (mL)	Malig-nancy	GTV (mL)	Image Dims	Voxel Dimensions (mm)
1	4.4	423	Eso ca.	25.9	256 × 256 × 112	1.16 × 1.16 × 2.50
2	3.5	406	Eso ca.	41.4	256 × 256 × 104	1.15 × 1.15 × 2.50
3	3.4	431	SCLC	211.1	512 × 512 × 120	0.97 × 0.97 × 2.50
4	2.4	191	Eso ca.	30.2	256 × 256 × 94	0.97 × 0.97 × 2.50
5	2.9	255	Eso ca.	54.1	512 × 512 × 128	0.97 × 0.97 × 2.50
6	5.4	635	Eso ca.	16.7	512 × 512 × 136	0.97 × 0.97 × 2.50

C= Case, RP= Respiratory period, TV=Tidal volume, Eso ca.= Esophagus cancer, SCLC= Small cell lung cancer, GTV= Gross tumour volume.

TABLE 2. Characteristics of landmarks for each case.

C	Land-mark num-ber	Average displacements (standard deviation) (mm)				
		IOE (mm)	3D Euclidean	AP	LR	SI
1	1487	0.70(0.99)	4.65(4.09)	0.72(0.88)	0.72(0.85)	4.09(4.37)
2	1166	1.13(1.27)	9.42(4.81)	1.28(1.23)	1.17(1.05)	6.10(4.49)
3	435	0.86(1.45)	7.63(6.54)	1.90(1.91)	0.93(0.91)	6.97(6.60)
4	1280	0.85(1.24)	4.01(2.91)	0.67(0.79)	0.58(0.62)	3.68(3.04)
5	342	0.75(1.09)	7.82(3.99)	2.98(1.93)	1.25(1.03)	6.45(4.51)
6	398	0.81(1.32)	11.59(7.87)	2.13(1.54)	1.28(1.17)	10.85(8.29)

IOE=Intra observer error, AP=anterior–posterior, LR=left–right, SI=superior–inferior.

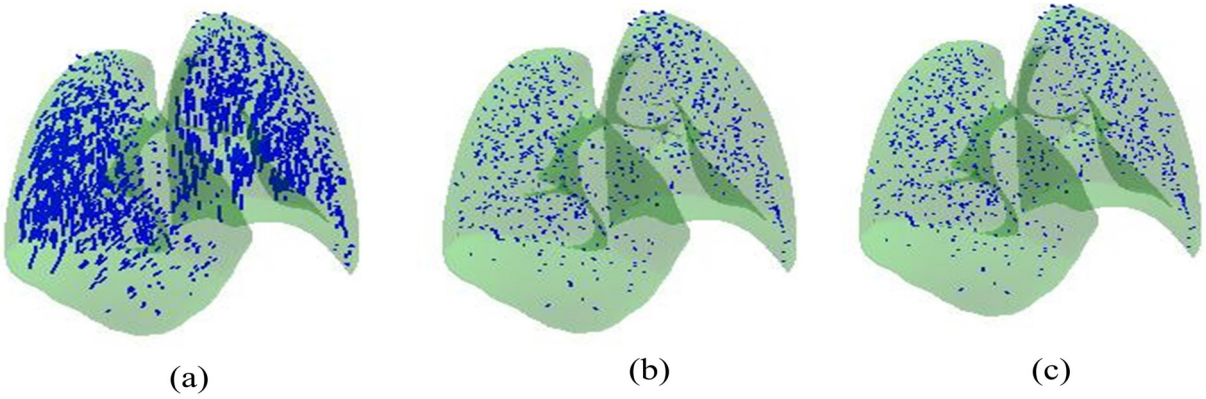

FIGURE 3. Error vectors of landmark points between T00 and T50 for case 2: (a) prior to registration, and after registration using (b) the Bayesian registration and (c) the proposed trajectory model.

TABLE 3. Spatial error in predicting lung motion using different methods.

Method	C	Average spatial error in predicting lung motion (mm)							
		3D Euclidean		LR		AP		SI	
		Mean	SD	Mean	SD	Mean	SD	Mean	SD
Linear	1	3.10	4.35	1.99	3.62	1.68	2.53	3.74	4.45
	2	4.05	6.26	1.91	3.45	1.53	5.59	2.59	6.68
	3	1.56	1.43	0.35	0.39	0.73	0.61	1.17	1.18
	4	2.79	6.97	2.36	8.95	1.78	10.95	4.45	9.03
	5	5.72	8.02	3.46	3.68	2.49	4.55	4.77	8.86
	6	4.96	4.53	1.54	1.63	1.52	1.66	3.94	4.41
	Average	3.70	5.26	1.94	3.62	1.62	4.32	3.44	5.77
Cosine	1	1.00	0.67	0.39	0.38	0.40	0.38	0.66	0.64
	2	1.34	0.89	0.53	0.48	0.63	0.57	0.83	0.82
	3	1.29	0.77	0.52	0.45	0.55	0.48	0.85	0.73
	4	1.33	0.89	0.44	0.39	0.64	0.61	0.89	0.81
	5	1.02	0.69	0.40	0.40	0.44	0.43	0.63	0.64
	6	1.49	0.94	0.56	0.53	0.66	0.56	0.98	0.89
	Average	1.25	0.81	0.47	0.44	0.55	0.51	0.81	0.76
Proposed	1	0.88	0.62	0.38	0.34	0.34	0.32	0.53	0.63
	2	1.11	0.67	0.40	0.34	0.42	0.35	0.80	0.68
	3	1.39	1.14	0.47	0.53	0.61	0.60	0.95	1.04
	4	0.93	0. 69	0.29	0.34	0.31	0.30	0.68	0.69
	5	0.99	0.67	0.40	0.39	0.44	0.44	0.59	0.62
	6	1.26	0.98	0.58	0.54	0.68	0.65	0.93	0.85
	Average	1.09	0.68	0.42	0.41	0.47	0.44	0.75	0.75

1.73 ± 1.28 mm and 1.55 ± 1.11 mm for the demons based method and the ANACONDA based method, which are reduced to 1.31 ± 0.74 mm and 1.22 ± 0.82 mm by the biomechanical model and the symmetric registration approach respectively. The proposed method achieves the lowest mean error ±SD of 1.09 ± 0.67mm, indicating that the proposed method is superior to the above four methods.

IV. DISCUSSION AND CONCLUSION

In this paper, we presented a novel approach for modelling the lung motion based on Bayesian registration and trajectory simulations. In the Bayesian registration, the neighbourhood information is combined with a similarity metric such that an initial displacement field is generated, which is smoothed and refined via the displacement regularisation. The dense displacement fields are then used to describe the lung motion.

TABLE 4. Spatial error for 300 landmarks when estimating lung motion using different methods.

C	Average spatial error in estimating lung motion (mm)									
	Demons based		ANACONDA based		Biomechanical model		Symmetric registration		Proposed	
	Mean	SD	Mean	SD	Mean	SD	Mean	SD	Mean	SD
1	1.08	0.60	0.94	0.67	0.99	0.49	1.01	0.62	0.89	0.61
2	1.90	1.30	1.59	1.24	1.49	0.99	1.39	0.96	1.12	0.65
3	2.02	2.10	2.03	1.51	1.41	0.84	1.23	0.88	1.39	1.13
4	1.05	0.60	1.01	0.56	1.08	0.55	1.19	1.01	0.92	0. 68
5	1.74	1.00	1.54	0.75	1.38	0.71	1.20	0.71	0.99	0.67
6	2.56	2.10	2.16	1.95	1.50	0.88	1.27	0.71	1.25	0.97
Average	1.73	1.28	1.55	1.11	1.31	0.74	1.22	0.82	1.09	0.67

This is achieved by linking the displacement field at the discrete phases using a continuous time-related polynomial function. The results indicate that the proposed method is superior to the linear-trajectory and cosine-trajectory models in predicting the motion of the lungs with a relatively high accuracy.

The proposed algorithm has provided encouraging results compared to some state-of-the-art image registration methods including the Demons based method, the ANACONDA based method, and the biomechanical model, as well as the symmetric registration approach. The Demons theory has been widely used for medical image registration, however, its assumption of intensity conservation disagrees with the fact that lung image intensity varies due to respiratory motion. The ANACONDA based method is found to have difficulty in handling with registration of images with large deformation (such as case 6). The biomechanical model provides physically realistic results, but its accuracy relies on model parameters such as Young's modulus, Poisson's ratio, friction coefficient and tissue heterogeneity, which are difficult to measure or estimate and thus limits application of the biomechanical model. Although the symmetric registration approach obtains accurate estimation of lung deformation, it is still not as accurate as the proposed method. It should be noted that these four previously published methods have been used to estimate deformation between images but unable to make prediction of lung motion between different states.

The proposed method is designed to construct spatiotemporal motion from 4DCT images. Specifically, Bayesian registration estimates spatial deformations of the lungs between discrete phases in respiratory cycle in the first stage, while the continuous motion is temporally recovered with trajectory modelling in the second stage. Different to the Bayesian model presented for reconstruction of 4DCT images in [31], the Bayesian registration in our study can tolerate intensity variation by introducing the neighborhood influence into data fidelity and lead to the smooth deformation by using the least median of squares as regularisation of displacement field. Generally, the proposed method not only can have a comparable registration performance to the four state-of-the-art deformable registration methods but also can predict the lung positions at any given time in a respiratory cycle.

Considering the predictive estimation of lung motion, the proposed method has potentials to be used in thoracic radiotherapy. For example, generic margins are often adopted based on population statistics for standard conformal radiotherapy, which may cause big margins used and increase toxicities to the surrounding normal tissues. By predicting lung motion along respiratory cycle, the proposed method makes it possible to generate individual-specific margins and to reduce treatment margins. As such, the dose to the normal tissues can be significantly reduced. Besides, patients' breathing causes the deformation and motion of lungs and tumours, which introduces difficulties in the target delineation and dose calculation. The proposed algorithm provides an alternative way to locate positions of lungs and tumours, which is beneficial for delineation of organs at risk and potentially improves accuracy of treatment for patients. In future work, we will apply the proposed method to develop the motion prediction model of patient-specific lung tumours, so that radiation oncologists can adjust the radiation treatment plan adaptively for precise radiation to tumours during radiotherapy.

In addition, the study has demonstrated the reasonability of the proposed method in prediction of lung motion during respiratory cycle. However, the number of the patients is small for experiment at present. Therefore, more patients will be enrolled to investigate the performance of our method in clinical settings in the future.

REFERENCES

[1] M. Li *et al.*, "Modeling lung deformation: A combined deformable image registration method with spatially varying Young's modulus estimates," *Med. Phys.*, vol. 40, no. 8, p. 081902, 2013.

[2] K. V. Tan *et al.*, "Predictors of respiratory-induced lung tumour motion measured on four-dimensional computed tomography," *Clin. Oncol.*, vol. 27, no. 4, pp. 197–204, 2015.

[3] A. J. Cole, G. G. Hanna, S. Jain, and J. M. O'Sullivan, "Motion management for radical radiotherapy in non-small cell lung cancer," *Clin. Oncol.*, vol. 26, no. 2, pp. 67–80, 2014.

[4] A. J. Cole *et al.*, "Investigating the potential impact of four-dimensional computed tomography (4DCT) on toxicity, outcomes and dose escalation for radical lung cancer radiotherapy," *Clin. Oncol.*, vol. 26, no. 3, pp. 142–150, 2014.
[5] A. Rasheed *et al.*, "Motion and volumetric change as demonstrated by 4DCT: The effects of abdominal compression on the GTV, lungs, and heart in lung cancer patients," *Pract. Radiat. Oncol.*, vol. 6, no. 5, pp. 352–359, 2016.
[6] P. Muyan-Ozcelik, J. D. Owens, J. Xia, and S. S. Samant, "Fast deformable registration on the GPU: A CUDA implementation of demons," in *Proc. Int. Conf. Comput. Sci. Appl.*, Perugia, Italy, Jun./Jul. 2008, pp. 223–233.
[7] R. Castillo *et al.*, "A framework for evaluation of deformable image registration spatial accuracy using large landmark point sets," *Phys. Med. Biol.*, vol. 54, no. 7, pp. 1849–1870, 2009.
[8] O. Lobachev, C. Ulrich, B. S. Steiniger, V. Wilhelmi, V. Stachniss, and M. Guthe, "Feature-based multi-resolution registration of immunostained serial sections," *Med. Image Anal.*, vol. 35, pp. 288–302, Jan. 2017.
[9] T. Verhoeven, X. Tong, R. Schreurs, S. Bergé, and T. Maal, "Quantification of facial asymmetry: A comparative study of landmark-based and surface-based registrations," *J. Cranio-Maxillofacial Surg.*, vol. 44, no. 9, pp. 1131–1136, 2016.
[10] M. Sergejeva *et al.*, "Anatomical landmarks for registration of experimental image data to volumetric rodent brain atlasing templates," *J. Neurosci. Methods*, vol. 240, pp. 161–169, Jan. 2015.
[11] S. Ghafurian, I. Hacihaliloglu, D. N. Metaxas, V. Tan, and K. Li, "A computationally efficient 3D/2D registration method based on image gradient direction probability density function," *Neurocomputing*, vol. 229, pp. 100–108, Mar. 2017.
[12] A. Valsecchi, S. Damas, J. Santamaría, and L. Marrakchi-Kacem, "Intensity-based image registration using scatter search," *Artif. Intell. Med.*, vol. 60, no. 3, pp. 151–163, 2014.
[13] K. Aghajani, M. T. Manzuri, and R. Yousefpour, "A robust image registration method based on total variation regularization under complex illumination changes," *Comput. Methods Program. Biomed.*, vol. 134, pp. 89–107, Oct. 2016.
[14] V. Gorbunova *et al.*, "Mass preserving image registration for lung CT," *Med. Image Anal.*, vol. 16, no. 4, pp. 786–795, 2012.
[15] A. Al-Mayah, J. Moseley, M. Velec, and K. Brock, "Toward efficient biomechanical-based deformable image registration of lungs for image-guided radiotherapy," *Phys. Med. Biol.*, vol. 56, no. 15, pp. 4701–4713, 2011.
[16] A. Pawar *et al.*, "Adaptive FEM-based nonrigid image registration using truncated hierarchical B-splines," *Comput. Math. Appl.*, vol. 72, no. 8, pp. 2028–2040, 2016.
[17] T. Hopp, N. Duric, and N. V. Ruiter, "Image fusion of ultrasound computer tomography volumes with X-ray mammograms using a biomechanical model based 2D/3D registration," *Comput. Med. Imag. Graph.*, vol. 40, pp. 170–181, Mar. 2015.
[18] G. Xiong, C. Chen, J. Chen, Y. Xie, and L. Xing, "Tracking the motion trajectories of junction structures in 4D CT images of the lung," *Phys. Med. Biol.*, vol. 57, no. 15, pp. 4905–4930, 2012.
[19] Z. Cao, E. Dong, Q. Zheng, W. Sun, and Z. Li, "Accurate inverse-consistent symmetric optical flow for 4D CT lung registration," *Biomed. Signal Process. Control*, vol. 24, pp. 25–33, Feb. 2016.
[20] Y. Yin, E. A. Hoffman, K. Ding, J. M. Reinhardt, and C. L. Lin, "A cubic B-spline-based hybrid registration of lung CT images for a dynamic airway geometric model with large deformation," *Phys. Med. Biol.*, vol. 56, no. 1, pp. 203–218, 2011.
[21] M. Li *et al.*, "Patient-specific biomechanical model as whole-body CT image registration tool," *Med. Image Anal.*, vol. 22, no. 1, pp. 22–34, 2015.
[22] T. Gass, G. Székely, and O. Goksel, "Simultaneous segmentation and multiresolution nonrigid atlas registration," *IEEE Trans. Image Process.*, vol. 23, no. 7, pp. 2931–2943, Jul. 2014.
[23] R. Castillo, E. Castillo, J. Martinez, and T. Guerrero, "Ventilation from four-dimensional computed tomography: Density versus jacobian methods," *Phys. Med. Biol.*, vol. 55, no. 16, pp. 4661–4685, 2010.
[24] E. Castillo, R. Castillo, B. White, J. Rojo, and T. Guerrero, "Least median of squares filtering of locally optimal point matches for compressible flow image registration," *Phys. Med. Bio.*, vol. 57, no. 15, pp. 4827–4833, 2012.
[25] D. Sarrut, V. Bolde, S. Miguet, and C. Ginestet, "Simulation of four-dimensional CT images from deformable registration between inhale and exhale breath-hold CT scans," *Med. Phys.*, vol. 33, no. 3, pp. 605–617, 2006.
[26] M. Li, L. Zhang, Z. Lian, Z. Xiang, and L. Xiao, "Estimation of lung motion using deformable image registration based on compressible flow," *J. Med. Imag. Health Inform.*, vol. 7, no. 7, pp. 1667–1670, 2017.
[27] B. W. Papiez, M. P. Heinrich, J. Fehrenbach, L. Risser, and J. A. Schnabel, "An implicit sliding-motion preserving regularisation via bilateral filtering for deformable image registration," *Med. Image Anal.*, vol. 18, no. 8, pp. 1299–1311, 2014.
[28] H. Miura *et al.*, "Impact of deformable image registration accuracy on thoracic images with different regularization weight parameter settings," *Phys. Med.*, vol. 42, pp. 108–111, 2017.
[29] L. Han, H. Dong, J. R. McClelland, L. Han, D. J. Hawkes, and D. C. Barratt, "A hybrid patient-specific biomechanical model based image registration method for the motion estimation of lungs," *Med. Image Anal.*, vol. 39, pp. 87–100, Jul. 2017.
[30] M. P. Heinrich, I. J. A. Simpson, B. W. Papież, M. Brady, and J. A. Schnabel, "Deformable image registration by combining uncertainty estimates from supervoxel belief propagation," *Med. Image Anal.*, vol. 27, pp. 57–71, Jan. 2016.
[31] T. He, Z. Xue, B. S. Teh, and S. T. Wong, "Reconstruction of four-dimensional computed tomography lung images by applying spatial and temporal anatomical constraints using a Bayesian model," *J. Med. Imag.*, vol. 2, no. 2, p. 024004, 2015.

MIN LI received the Ph.D. degree in biomedical engineering from Chongqing University in 2014. From 2011 to 2013, she was a Visiting Ph.D. Student with the Department of Radiation Oncology, University of Texas MD Anderson Cancer Center, Houston, TX, USA. She is currently an Assistant Professor with the School of Computer Science and Engineering, Nanjing University of Science and Technology. Her current research interests include medical image processing, analysis, and visualization.

ZHIKANG XIANG received the B.S. degree from the Nanjing University of Agriculture in 2015. He is currently pursuing the Ph.D. degree with the School of Computer Science and Engineering, Nanjing University of Science and Technology. His research interests include image registration and segmentation.

ZHICHAO LIAN is currently an Associate Professor with the School of Computer Science and Engineering, Nanjing University of Science and Technology. His current research interests include medical image processing and motion tracking.

LIANG XIAO (M'11) is currently a Professor with the School of Computer Science and Engineering, Nanjing University of Science and Technology. His research interests include pattern recognition, image processing, virtual reality, and system simulation.

JUN ZHANG is currently an Associate Professor with the School of Science, Nanjing University of Science and Technology. His research interests include image modeling and variational partial differential equation application in image processing.

ZHIHUI WEI is currently a Professor with the School of Computer Science and Engineering, Nanjing University of Science and Technology. His research interests include image processing, image modeling, wavelet analysis, digital watermark, and image coding and compressing.